Electronic Supplementary Material (ESI) for Journal of Materials Chemistry A.

Supporting Information

Ultramicroporous Carbon Aerogel Encapsulating Sulfur as Cathode for Lithium-Sulfur Batteries

Maryam Nojabaee[*a], *Brigitta Sievert*[a], *Marina Schwan*[b], *Jessica Schettler*[b], *Frieder Warth*[a], *Norbert Wagner*[a], *Barbara Milow*[b,c], *K. Andreas Friedrich*[a,d]

[a]German Aerospace Center (DLR), Institute of Engineering Thermodynamics, Stuttgart, Germany
[b]German Aerospace Center (DLR), Institute of Material Research, Cologne, Germany
[c]University of Cologne, Institute of Inorganic Chemistry, Cologne, Germany
[d]University of Stuttgart, Institute for Building Energetics, Stuttgart, Germany

The conductivity of the CA(N_2/CO_2) slightly higher than that of a CA(Ar) at higher pressures, Figure S1.

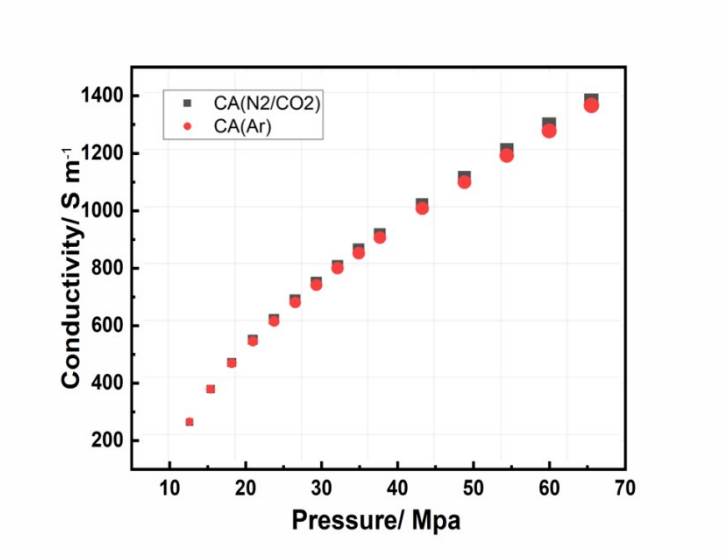

Figure S1 The electrical conductivity of carbon aerogels measured at different pressures using 4 point measurement technique.

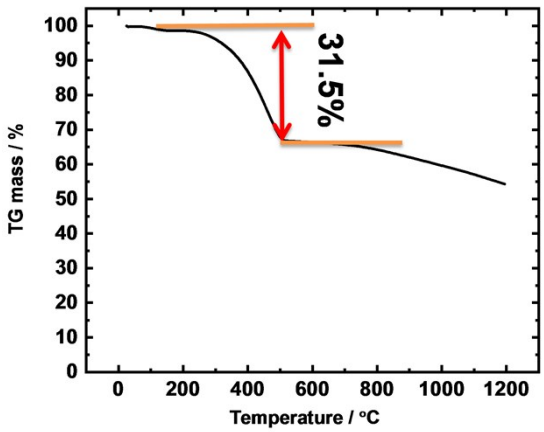

Figure S 2 TGA measurements of CA(N_2/CO_2)+S_{inf} .

The higher volume of micropores in CA(N_2/CO_2) samples results in infiltration of higher percentage of the active material, Figure S2.

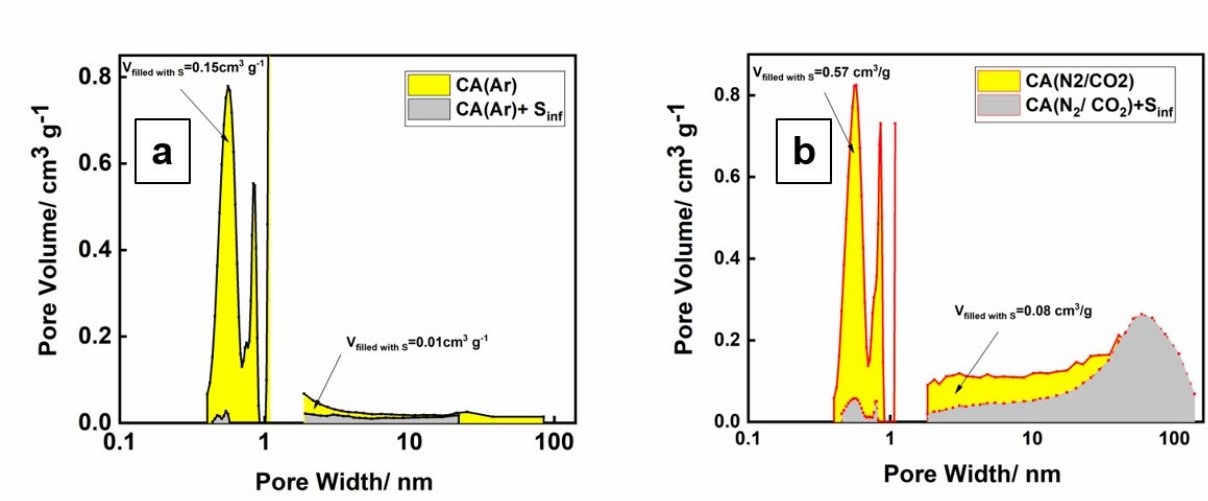

Figure S3 N_2-isotherms before and after infiltration of a) CA(Ar) b) CA(N_2/CO_2).

The mass of sulfur which can be accommodated by the micropores according to its mass fraction can be calculated by

$$w_S = \frac{m_S}{m} = \frac{m_S}{m_S + m_{CA}} = \frac{(V_{MP} \times \rho_S)}{(V_{MP} \times \rho_S) + m_{CA}} \quad (1)$$

where m_S and m_{CA} are the mass of sulfur and CA, V_{MP} is the micropore volume, determined by N_2-physisorption, and ρ_S is the theoretical density of sulfur of 2.06 g cm^{-3}. This results in a sulfur mass fraction of 27 wt.-%, which corresponds well with the mass loss of sulfur during the TGA measurement for CA(Ar) sample which is about 25 wt.-% and proves that the sulfur is accommodated in the micropores leaving additional pore space of 15 vol.-%.

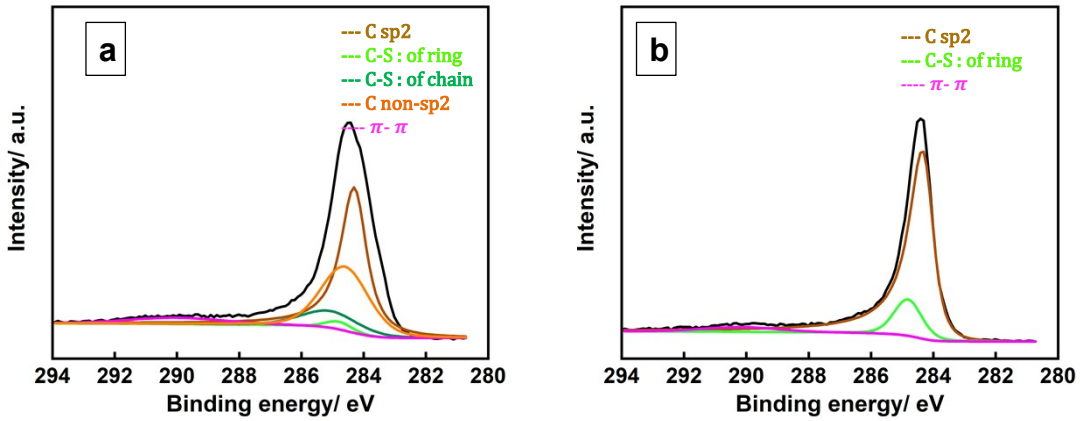

Figure S4 C 1s signal of the recorded XPS spectra for a) CA(Ar)+S_{inf} b) CA(N_2/CO_2)+S_{inf}

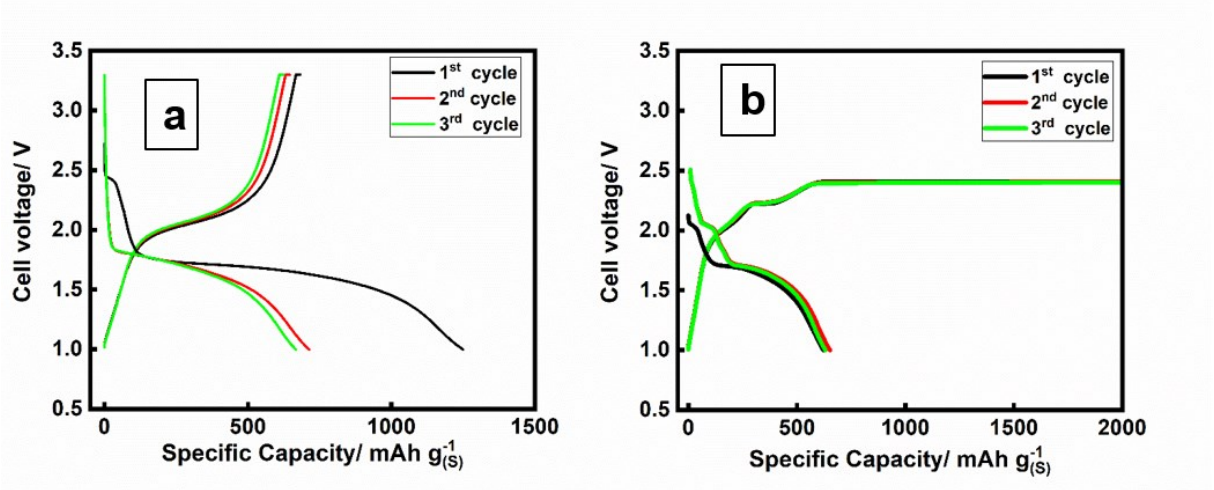

Figure S5 The charge-discharge profiles of the formation phase at 0.1C rate for CA(Ar)+S_{mix} in a) carbonate electrolyte b) ether electrolyte.

CA(Ar)+S_{mix} in carbonate electrolyte, Figure S5a shows a fully active quasi-solid-state conversion reaction despite the lack of gas-infiltration techniques. CA(Ar)+S_{mix} , Figure S5b reveals a stark polysulfide shuttle upon charge, albeit the activation of lower plateau in discharge.

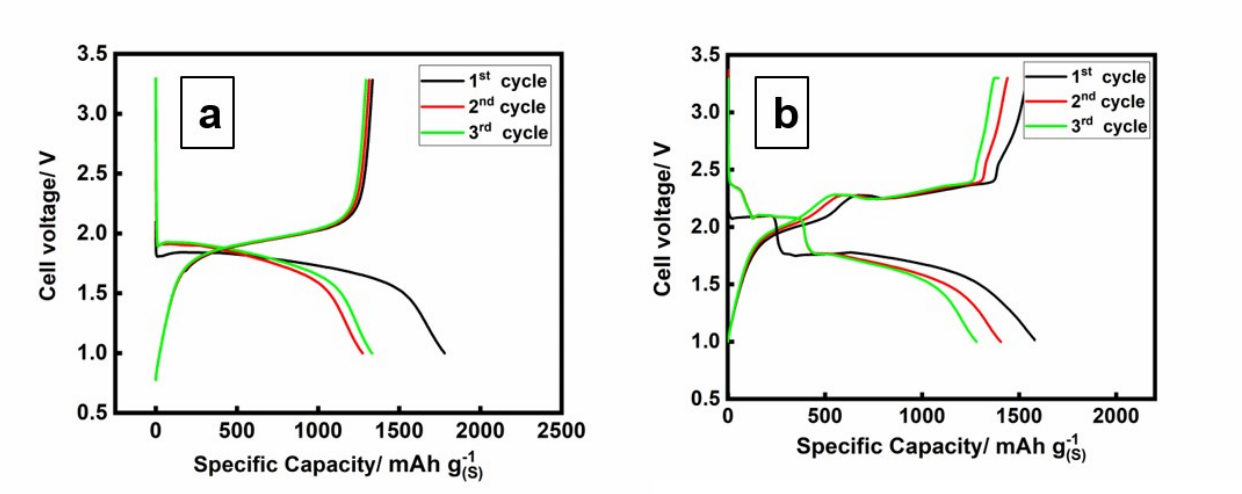

Figure S6 The charge-discharge profiles of the formation phase at 0.1C rate of CA(N_2/CO_2)+S_{inf} for a)carbonate electrolyte b)ether electrolyte.

CA(N_2/CO_2)+S_{inf} , Figure S6c, has an analogous discharge-charge behavior to the CA(Ar)+S_{inf} , explained in the main manuscript.

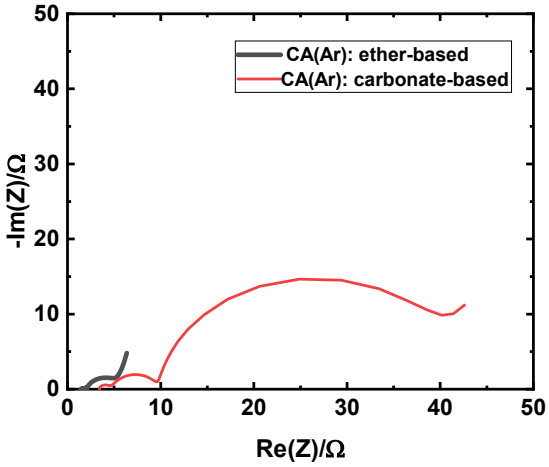

Figure S7 Impedance spectra of symmetrical CA(Ar)+S_{inf} sulfur electrode in carbonate and ether-based electrolyte at 100% depth of discharge.

The additional semi-circle in mid-frequency regime after fully discharge (100% DoD) of the cathode is still visible. Low-frequency semi-circle is assigned to the charge transfer processes which shows clearly higher value of resistance. The future work will address the impedance spectroscopy of such cathodes in details.

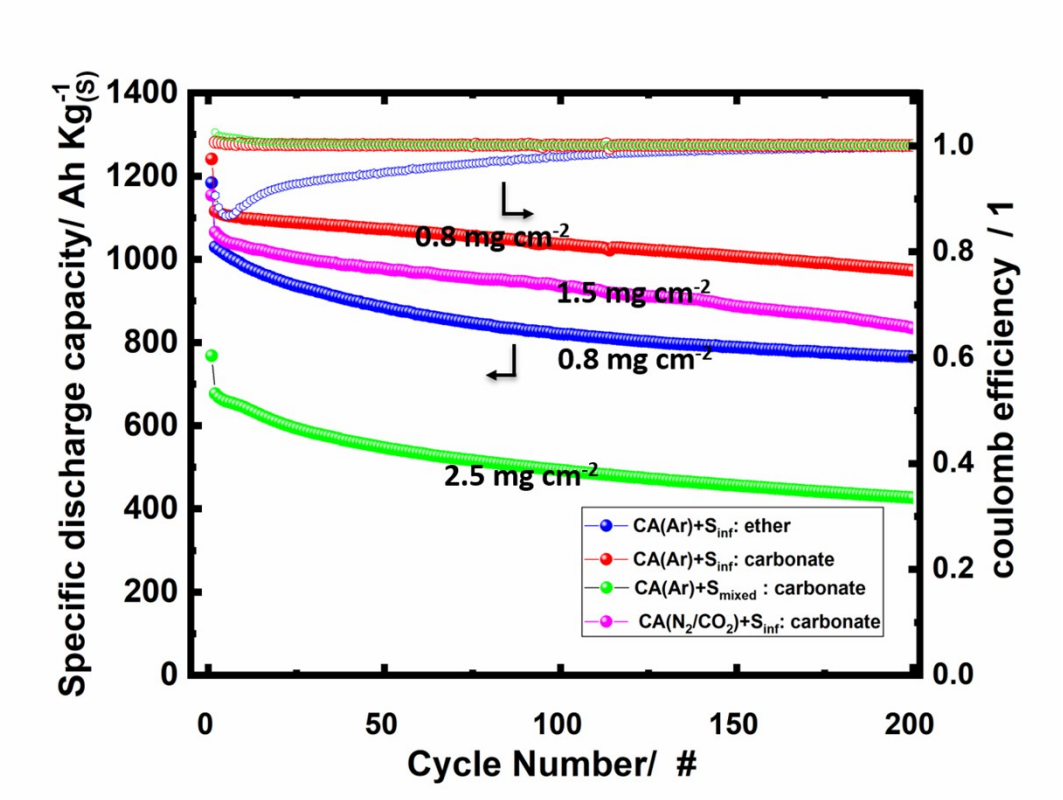

Figure S8 Discharge capacity and coulomb efficiency as a function of cycle number at 0.3 C rate for: CA(Ar)+Sinf in ether electrolyte (blue), carbonate electrolyte(red), CA(N2/CO2)+Sinf with the loading of 1.5 mg cm-2 in carbonate electrolyte (purple) and CA(Ar)+Smixed in carbonate electrolyte (green).